J. Appl. Comput. Mech., 10(1) (2024) 55-63
DOI: 10.22055/jacm.2023.44219.4182

ISSN: 2383-4536
jacm.scu.ac.ir

Shahid Chamran University of Ahvaz

Journal of Applied and Computational Mechanics

Research Paper

Influence of Discretely Introduced Cutouts on the Buckling of Shallow Shells with Double Curvature

Nikolai Mishurenko, Alexey Semenov

Department of Computer Science, Saint Petersburg State University of Architecture and Civil Engineering, 4, 2nd Krasnoarmeyskaya st., Saint-Petersburg, 190005, Russia, Email: nikolai8421@mail.ru (N.M.); sw.semenov@gmail.com (A.S.)

Received July 05 2023; Revised August 23 2023; Accepted for publication September 03 2023.
Corresponding author: N. Mishurenko (nikolai8421@mail.ru)

Abstract. The paper analyzes the influence of cutouts on the buckling of shallow shells with double curvature. Based on the Timoshenko-Reissner hypothesis, a mathematical model is presented that considers transverse shifts, material orthotropy, geometric nonlinearity and structural weakening by cutouts. Cutouts are specified discretely by single columnar functions. The computational algorithm is based on the Ritz method and the Newton method. The implementation of the algorithm is carried out in the Maple 2022 software package. To study the buckling, the Lyapunov criterion is adopted. Calculations of the buckling of flat shells of double curvature with square cuts, graphs of the dependence of deflections on loads and deflection fields are given. Accounting for the structural cutouts leads to a decrease in the critical load. At the same time, for the considered problems, it is found that the decrease in the critical load does not exceed 25 % for the cutout volume not exceeding 10 % of the shell volume.

Keywords: Shells, cutouts, buckling, critical load, Ritz method, Newton method.

1. Introduction

Shell structures are used in many areas of industry such as shipbuilding, aircraft building, space building and construction [1–3]. In industrial construction, tanks, gas tanks, silos, etc. are made from shell structures; in civil engineering, shells are used, if necessary, for large spans (stadiums, opera houses, airports, shopping centers). In addition, shell structures are used in bridge building, hydraulic engineering (in the construction of offshore berthing and protective structures), and in the construction of nuclear power plants. At the same time, it should be noted that, often, for structural reasons, it is necessary to arrange technological cutouts that affect the stress-strain state and buckling of the structure. In this regard, there is a need to study such structures.

There are various mathematical models of shells weakened by cutouts, among which it should be noted: the method of constructive anisotropy and the discrete introduction of attenuations using unit column functions [4, 5]. Kamenev and Semenov [4] demonstrated that with a large number of notches, the discreteness of their input is lost and it becomes possible to use the constructive anisotropy method. The effect of weakening on nonlinear deformation and buckling using the finite element moment scheme and software packages LIRA and SCAD was presented by Solovei et al. [6]. Zakharova and Lokhmatova [7] proposed a mathematical model for the deformation of cylindrical shells made of composite materials with defects, based on the Timoshenko model, using the finite element method. The effect of geometric imperfections on the buckling of cylindrical shells under compression based on the results of laboratory and computational experiments was presented by Zhao et al. [8]. Dmitriev et al. [9] presented the mathematical models and numerical methods for studying the nonlinear deformation and buckling of cylindrical shells, considering rectangular cutouts. Dmitriev et al. [10] presented a method for the analytical calculation of cylindrical shells with cutouts, obtained by the authors based on the convergence of the results of numerical simulation in ABAQUS and experiments. An isogeometric analysis using the discontinuous Galerkin method for the peridynamic approach for modeling cracks in shell structures was studied by Xia et al. [11]. Ambati et al. [12] proposed the use of a “mixed” model for modeling cracks in structures, which combined the structural elements that represent the displacement field in the two-dimensional middle surface of the shell, with continuum elements that describe the phase field of cracks in three-dimensional solid space. The effect of defects and microcracks on free vibrations of cylindrical shells was examined by Wang et al. [13]. Estimation of the parameters of perforation of cylindrical shells for free vibrations was studied by Giani and Hakula [14].

The work conducted by Arbelo et al. [15] was devoted to the influence of cutouts on the value of the critical load, considering the geometric imperfections of the structure. According to the results of Gangadhar and Kumar [16], it was found that the geometry of cutouts has a significant impact on the critical load of cylindrical shells: the maximum value of the critical load for the arrangement of round cutouts, the minimum value of the critical load for a structure with rectangular cutouts.

An experimental study of the buckling and post-buckling behavior of perforated cylindrical shells subjected to hydrostatic pressure was presented by Shen et al. [17]. Ghanbari Ghazijahani et al. [18] carried out an experimental assessment of the effect of cutouts on cylindrical shells and the effectiveness of reinforcement: the introduction of stiffeners made it possible to reduce the effect of cutouts by 33 %. A comprehensive assessment of the effect of fiberglass reinforcement of steel cylindrical shells, considering the weakening was examined by Krishna et al. [19]. Sohan et al. [20] conducted an assessment of the effect of cutouts on the buckling and bearing capacity of a rectangular plate reinforced with stiffeners. According to the results of the study, it was found that the strength of an isotropic panel decreases when cutouts are included and directly depends on the size/area of the cutouts; for composite panels, the dependence of strength reduction on the geometric parameters of cutouts was not revealed.

An assessment of the impact of oval cutouts on the buckling and stress distribution in rectangular plates was presented by da Silveira et al. [21]. The effect of cutouts on the buckling and load-bearing capacity of multilayer composite cylindrical panels subjected to impulse loads was investigated by Keshav et al. [22]. It was found that for structures with cutouts, the dynamic buckling load is, in some cases, lower than the static buckling load. Dewangan et al. [23] proposed a finite element model based on high-order shear deformation theory (HSDT) for the static analysis of cutouts composite shells. The application of this finite element model made it possible to reveal the relationship between the curvature and deflection of a structure with a cutout: an increase in curvature leads to an increase in the deflection of the considered shells. Dewangan et al. [24] investigated the static and dynamic deformation of composite shells with cutouts under thermomechanical action for various geometric shapes (plate, cylindrical shell, spherical shell, etc.).

When reviewing scientific research devoted to the study of the effect of weakening on the stress-strain state (SSS) of a structure over the past ten years, it can be noted that considerable attention was focused on the study of cylindrical shells [25–27]. Studies of the supercritical behavior of weakened cylindrical shells were presented in [28, 29]. At the same time, the SSS weakening of shells of other shapes, for example, conical [30, 31] and spherical [32, 33], was also evaluated.

Based on a review of the literature, it can be concluded that determining the effect of cutouts on the stress-strain state and buckling of shells is an urgent task. The purpose of this work is to analyze the buckling of shallow shells of double curvature, considering the presence of notches. The objectives of the study are: development of a mathematical model that simultaneously considers geometric nonlinearity, transverse shifts, orthotropy of the material, weakening of the structure by cutouts; selection of an algorithm that allows one to study the buckling of shell structures; writing a program code designed to implement the selected algorithm. The resulting mathematical model and algorithm will allow to investigate the stress-strain state and buckling of shell structures with cutouts with greater accuracy. The use of the proposed technique will provide an opportunity to evaluate the effect of structural weakening by cutouts on the buckling of shells. Based on this assessment, make decisions on the need to strengthen these structures.

2. Theory and Methods

2.1 Mathematical Model

Thin-walled flat shells of double curvature, weakened by cutouts, under the action of a static load are considered. The geometric appearance of these shell structures is characterized by the Lame parameters A, B and the radii of the main curvatures R_1, R_2 along the coordinates x, y, respectively. For shallow shells of double curvature (Fig. 1), $A = 1, B = 1$, $R_1 = const, R_2 = const$.

The mathematical model of Timoshenko-Reisner is used, which considers transverse shifts, geometric nonlinearity, orthotropy. According to this model, three displacement functions $U = U(x,y), V = V(x,y), W = W(x,y)$ and two functions characterizing the angles of rotation of the normal in the planes are unknown $xOz, yOz : \Psi_x(x,y), \Psi_y(x,y)$. The stability of the shell can be studied by considering the geometric nonlinearity [34].

The basis of the model used is the functional of the total potential energy of deformation, which can be represented in the following form:

$$E_s = E_s^0 + E_s^V, \tag{1}$$

where E_s^0 is the functional of the total potential energy of the deformation of the shell skin, E_s^V is the functional of the total potential energy of the deformation of cutouts.

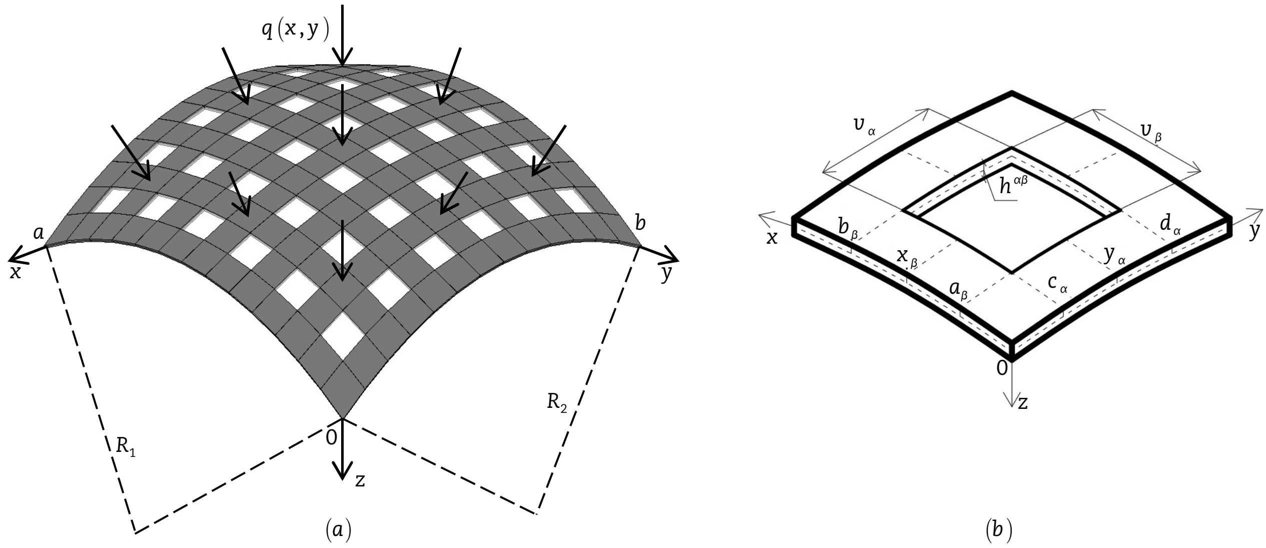

Fig. 1. Shallow shell with double curvature: (a) Design scheme; (b) Cutout geometry.

The functional of the total potential energy of deformation of the shell skin has the following form:

$$E_s^0 = \frac{1}{2}\int_{a_1}^{a}\int_{0}^{b}\Big[N_x^0\varepsilon_x + N_y^0\varepsilon_y + \frac{1}{2}\left(N_{xy}^0 + N_{yx}^0\right)\gamma_{xy} + M_x^0\chi_1 + M_y^0\chi_2 + \left(M_{xy}^0 + M_{yx}^0\right)\chi_{12} + Q_x^0\left(\Psi_x - \theta_1\right) + Q_y^0\left(\Psi_y - \theta_2\right) - 2P_xU - 2P_yV - 2qW\Big]ABdxdy. \tag{2}$$

Here q, P_x, P_y are the load components; N_x^0, N_y^0 are normal forces in the direction of the axes x, y; N_{xy}^0, N_{yx}^0 – shear forces in the corresponding plane xOy; M_x^0, M_y^0 – bending moments; M_{xy}^0, M_{yx}^0 – torques; Q_x^0, Q_y^0 – transverse forces in the planes xOz and xOy, which are determined by the relations [35]:

$$N_x^0 = \frac{E_1 h}{1-\mu_{12}\mu_{21}}\left(\varepsilon_x + \mu_{21}\varepsilon_y\right), \quad N_y^0 = \frac{E_2 h}{1-\mu_{12}\mu_{21}}\left(\varepsilon_y + \mu_{12}\varepsilon_x\right), \; N_{xy}^0 = N_{yx}^0 = G_{12}h\gamma_{xy},$$

$$M_x^0 = \frac{E_1 h^3}{12\left(1-\mu_{12}\mu_{21}\right)}\left(\chi_1 + \mu_{21}\chi_2\right), \quad M_y^0 = \frac{E_2 h^3}{12\left(1-\mu_{12}\mu_{21}\right)}\left(\chi_2 + \mu_{21}\chi_1\right), \quad M_{xy}^0 = M_{yx}^0 = \frac{G_{12}h^3}{6}\chi_{12}, \tag{3}$$

$$Q_x^0 = G_{13}kh\left(\Psi_x - \theta_1\right), Q_y^0 = G_{23}kh\left(\Psi_y - \theta_2\right).$$

The functional of the total potential strain energy of shell cutouts has the following form:

$$E_s^V = \frac{1}{2}\int_{a_1}^{a}\int_{0}^{b}\Big[N_x^V\varepsilon_x + N_y^V\varepsilon_y + \frac{1}{2}\left(N_{xy}^V + N_{yx}^V\right)\gamma_{xy} + M_x^V\chi_1 + M_y^V\chi_2 + \left(M_{xy}^V + M_{yx}^V\right)\chi_{12} + Q_x^V\left(\Psi_x - \theta_1\right) + Q_y^V\left(\Psi_y - \theta_2\right)\Big]ABdxdy, \tag{4}$$

where the forces and moments in the cutout areas take the following form:

$$N_x^V = \frac{E_1}{1-\mu_{12}\mu_{21}}\left(\bar{F}_V\left(\varepsilon_x + \mu_{21}\varepsilon_y\right) + \bar{S}_V\left(\chi_1 + \mu_{21}\chi_2\right)\right), \quad N_y^V = \frac{E_2}{1-\mu_{12}\mu_{21}}\left(\bar{F}_V\left(\varepsilon_y + \mu_{12}\varepsilon_x\right) + \bar{S}_V\left(\chi_2 + \mu_{12}\chi_1\right)\right),$$

$$N_{xy}^V = N_{yx}^V = G_{12}\left[\bar{F}_V\gamma_{xy} + 2\bar{S}_V\chi_{12}\right],$$

$$M_x^V = \frac{E_1}{1-\mu_{12}\mu_{21}}\left[\bar{S}_V\left(\varepsilon_x + \mu_{21}\varepsilon_y\right) + \bar{J}_V\left(\chi_1 + \mu_{21}\chi_2\right)\right], \quad M_y^V = \frac{E_2}{1-\mu_{12}\mu_{21}}\left[\bar{S}_V\left(\varepsilon_y + \mu_{12}\varepsilon_x\right) + \bar{J}_V\left(\chi_2 + \mu_{12}\chi_1\right)\right], \tag{5}$$

$$M_{xy}^V = M_{yx}^V = G_{12}\left[\bar{S}_V\gamma_{xy} + 2\bar{J}_V\chi_{12}\right],$$

$$Q_x^V = G_{13}k\bar{F}_V\left(\Psi_x - \theta_1\right), \; Q_y^V = G_{23}k\bar{F}_V\left(\Psi_y - \theta_2\right).$$

Here, E_1, E_2 are the elastic moduli in the directions x, y; $k = 5/6$; G_{12}, G_{13}, G_{23} are shear moduli in planes xOy, xOz, yOz, respectively; μ_{12}, μ_{21} are Poisson's ratios; $\varepsilon_x, \varepsilon_y$ – elongation deformations; γ_{xy} – shear deformations in the plane xOy; $\chi_1, \chi_2, \chi_{12}$ – functions for changing curvatures and torsion [35]:

$$\varepsilon_x = \frac{1}{A}\frac{\partial U}{\partial x} + \frac{1}{AB}V\frac{\partial A}{\partial y} - k_xW + \frac{1}{2}\theta_1^2, \; \varepsilon_y = \frac{1}{B}\frac{\partial V}{\partial y} + \frac{1}{AB}U\frac{\partial B}{\partial x} - k_yW + \frac{1}{2}\theta_2^2,$$

$$\gamma_{xy} = \frac{1}{A}\frac{\partial V}{\partial x} + \frac{1}{B}V\frac{\partial U}{\partial y} - \frac{1}{AB}U\frac{\partial A}{\partial y} - \frac{1}{AB}\frac{\partial B}{\partial x}V + \theta_1\theta_2,$$

$$\theta_1 = -\left(\frac{1}{A}\frac{\partial W}{\partial x} + k_xU\right), \qquad \theta_2 = -\left(\frac{1}{B}\frac{\partial W}{\partial y} + k_yV\right), \tag{6}$$

$$\chi_1 = \frac{1}{A}\frac{\partial \Psi_x}{\partial x} + \frac{1}{AB}\frac{\partial A}{\partial y}\Psi_y, \qquad \chi_2 = \frac{1}{B}\frac{\partial \Psi_y}{\partial y} + \frac{1}{AB}\frac{\partial B}{\partial x}\Psi_x, \qquad \chi_{12} = \frac{1}{2}\left(\frac{1}{A}\frac{\partial \Psi_y}{\partial x} + \frac{1}{B}\frac{\partial \Psi_y}{\partial x} - \frac{1}{AB}\left(\frac{\partial A}{\partial y}\Psi_y + \frac{\partial B}{\partial x}\Psi_y\right)\right).$$

The areas of location of shell cutouts are specified by the function [5]:

$$H^V(x,y) = -\sum_{\alpha=1}^{o}\sum_{\beta=1}^{p}h^{\alpha\beta}\bar{\delta}\left(x - x_\beta\right)\bar{\delta}\left(y - y_\alpha\right), \tag{7}$$

where $h^{\alpha\beta}$ is the thickness of the notch; α, β indices indicate the number of a rectangular cutout, the sides of which are parallel to the x and y axes; o, p – number of cutouts along the x and y axes, respectively; $\bar{\delta}\left(x - x_\beta\right), \bar{\delta}\left(y - y_\alpha\right)$ are single columnar functions that are equal to one at the place where there is a notch and equal to zero outside of such places.

Thus, the thickness of the entire structure is equal to $h + H^V$.

It is noted in [4,5] that unit column functions are equally suitable for considering structural weakening and reinforcements with ribs. In this connection, approaches that consider the effect of stiffeners will be valid for considering the effect of weakening. Thus, the geometric characteristics and the functional of the total potential energy of the deformation of cutouts are determined according to [5,35].

Integrating the function $H^V(x,y)$ over z in the range from $h/2$ to $h/2 + H^V$ obtain the stiffness functions of the cutouts:

$$\int_{h/2}^{h/2+H^V} dz = \bar{F}_V = -\sum_{\alpha=1}^{o}\sum_{\beta=1}^{p}F_V^{\alpha\beta}\bar{\delta}\left(x - x_\beta\right)\bar{\delta}\left(y - y_\alpha\right), \tag{8}$$

$$\int_{h/2}^{h/2+H^V} z dz = \bar{S}_V = -\sum_{\alpha=1}^{o}\sum_{\beta=1}^{p} S_V^{\alpha\beta}\bar{\delta}(x-x_\beta)\bar{\delta}(y-y_\alpha),$$
$$\int_{h/2}^{h/2+H^V} z^2 dz = \bar{J}_V = -\sum_{\alpha=1}^{o}\sum_{\beta=1}^{p} J_V^{\alpha\beta}\bar{\delta}(x-x_\beta)\bar{\delta}(y-y_\alpha), \tag{8-cont.}$$

where $\bar{F}_V, \bar{S}_V, \bar{J}_V$ are the functions characterizing the area, static moment and moment of inertia of cutouts:

$$F_V^{\alpha\beta} = h^{\alpha\beta}, \quad S_V^{\alpha\beta} = \frac{h^{\alpha\beta}\left(h+h^{\alpha\beta}\right)}{2}, \quad J_V^{\alpha\beta} = 0{,}25h^2h^{\alpha\beta} + 0{,}5h\left(h^{\alpha\beta}\right)^2 + \frac{1}{3}\left(h^{\alpha\beta}\right)^3. \tag{9}$$

The functional of the total potential energy of deformation of cutouts takes the form [35]:

$$E_s^V = -\sum_{\alpha=1}^{o}\sum_{\beta=1}^{p}\int_{a_\beta}^{b_\beta}\int_{c_\alpha}^{d_\alpha} B_{\alpha\beta} dxdy, \tag{10}$$

where:

$$\begin{aligned} B_{\alpha\beta} = \Big[& G_1\left(F_V^{\alpha\beta}\left(\varepsilon_x + \mu_{21}\varepsilon_y\right)\varepsilon_x + S_V^{\alpha\beta}\left(\chi_1 + \mu_{21}\chi_2\right)\varepsilon_x\right)\upsilon_a + G_2\left(F_V^{\alpha\beta}\left(\varepsilon_y + \mu_{12}\varepsilon_x\right)\varepsilon_y + S_V^{\alpha\beta}\left(\chi_2 + \mu_{12}\chi_1\right)\varepsilon_y\right)\upsilon_b + \\ &+ G_{12}\left(F_V^{\alpha\beta}\gamma_{xy}^2 + 2S_V^{\alpha\beta}\chi_{12}\gamma_{xy}\right)\upsilon_{ab} + G_1\left(S_V^{\alpha\beta}\left(\varepsilon_x + \mu_{21}\varepsilon_y\right)\chi_1 + J_V^{\alpha\beta}\left(\chi_1 + \mu_{21}\chi_2\right)\chi_1\right)\upsilon_a + G_2\left(S_V^{\alpha\beta}\left(\varepsilon_y + \mu_{12}\varepsilon_x\right)\chi_2 + \right. \\ &\left. + J_V^{\alpha\beta}\left(\chi_2 + \mu_{12}\chi_1\right)\chi_2\right)\upsilon_b + 2G_{12}\left(S_V^{\alpha\beta}\gamma_{xy}\chi_{12} + 2J_V^{\alpha\beta}\chi_{12}^2\right)\upsilon_{ab} + G_{13}k\left(\Psi_x - \theta_1\right)^2 F_V^{\alpha\beta}\upsilon_a + G_{23}k\left(\Psi_y - \theta_2\right)^2 F_V^{\alpha\beta}\upsilon_b\Big]AB, \end{aligned} \tag{11}$$

here:

$$\upsilon_a = \frac{\upsilon_\beta}{aA}, \upsilon_b = \frac{\upsilon_\alpha}{bB}, \upsilon_{ab} = \frac{\upsilon_a + \upsilon_b}{2}, \tag{12}$$

where $\upsilon_\alpha, \upsilon_\beta$ are the widths of cutouts in the x, y directions, respectively.

2.2 Algorithm for the Solution of Buckling Problems

To study the stability of the shell structure, it is required to find the minimum of the functional (1). Use the Ritz method to reduce the variational problem of finding the minimum of a functional to solving a system of nonlinear algebraic expressions. Represent the unknown functions in the form:

$$\begin{gathered} U = U(x,y) = \sum_{k=1}^{\sqrt{N}}\sum_{l=1}^{\sqrt{N}} U_{kl}X_1^kY_1^l, \qquad V = V(x,y) = \sum_{k=1}^{\sqrt{N}}\sum_{l=1}^{\sqrt{N}} V_{kl}X_2^kY_2^l, \qquad W = W(x,y) = \sum_{k=1}^{\sqrt{N}}\sum_{l=1}^{\sqrt{N}} W_{kl}X_3^kY_3^l, \\ \Psi_x = \Psi_x(x,y) = \sum_{k=1}^{\sqrt{N}}\sum_{l=1}^{\sqrt{N}} \Psi_{xkl}X_4^kY_4^l, \qquad \Psi_y = \Psi_y(x,y) = \sum_{k=1}^{\sqrt{N}}\sum_{l=1}^{\sqrt{N}} \Psi_{ykl}X_5^kY_5^l, \end{gathered} \tag{13}$$

where $U_{kl}, V_{kl}, W_{kl}, \Psi_{x_{kl}}, \Psi_{y_{kl}}$ are unknown numerical parameters; $X_1^k,..., X_5^k$ and $Y_1^l,..., Y_5^k$ are known approximating functions that satisfy the boundary conditions. Boundary conditions are assigned based on the method of fixing the structure contour.

Thin-walled flat shells of double curvature, hinged-fixed along the contour (at $x = a_1 = 0, x = a$: $U = V = W = M_x = \Psi_y = 0$; at $y = 0, y = b$: $U = V = W = M_y = \Psi_x = 0$) are considered. In this case, the following trigonometric functions can be used as approximating functions:

$$\begin{aligned} X_1^k &= \sin\left(2k\pi\frac{x-a_1}{a-a_1}\right), \quad Y_1^l = \sin\left((2l-1)\pi\frac{y}{b}\right), \\ X_2^k &= \sin\left((2k-1)\pi\frac{x-a_1}{a-a_1}\right), \quad Y_2^l = \sin\left(2l\pi\frac{y}{b}\right), \\ X_3^k &= \sin\left((2k-1)\pi\frac{x-a_1}{a-a_1}\right), \quad Y_3^l = \sin\left((2l-1)\pi\frac{y}{b}\right), \\ X_4^k &= \cos\left((2k-1)\pi\frac{x-a_1}{a-a_1}\right), \quad Y_4^l = \sin\left((2l-1)\pi\frac{y}{b}\right), \\ X_5^k &= \sin\left((2k-1)\pi\frac{x-a_1}{a-a_1}\right), \quad Y_5^l = \cos\left((2l-1)\pi\frac{y}{b}\right). \end{aligned} \tag{14}$$

After substituting Eq. (14) into Eq. (1), derivatives with respect to unknown numerical parameters are found and equated to zero. Thus, a system of nonlinear algebraic equations has been obtained. The solution of this system is carried out by Newton's method.

The implementation of this algorithm is carried out in the Maple mathematical package. In this work, the Lyapunov buckling criterion is used: a small change in the input parameter (load q) corresponds to a significant change in the output parameter (displacement W).

When studying the buckling of shells with a successive increase in the value of the load, an iterative problem is solved and a graph of the dependence of the deflection W on the load q at a point of the structure is constructed. The load corresponding to the extremum of this dependence is assumed to be critical q_{cr}. When this load is reached, a jump to a new equilibrium state occurs.

Table 1. Considered shallow shells of double curvature.

No	h, m	a, m	b, m	R_1, m	R_2, m
1	0.09	54	54	135.9	135.9
2	0.09	18	18	45.27	45.27
3	0.09	10.8	10.8	40.05	40.05

Table 2. Critical loads for shallow shells of double curvature with cutouts.

No	N	Critical buckling load q_{cr}, MPa							
		0×0	1×1	2×2	3×3	4×4	5×5	6×6	7×7
1	9	0.09	0.09	0.09	0.09	0.08	0.07	0.07	0.06
	16	0.07	0.07	0.07	0.06	0.06	0.05	0.02	0.012
2	9	0.64	0.64	0.64	0.59	0.48	0.22	0.28	0.13
	16	0.59	0.59	0.54	0.49	0.39	0.21	0.14	0.12
3	9	0.79	0.78	0.71	0.62	0.59	0.3	0.4	0.08
	16	0.78	0.78	0.66	0.6	0.53	0.24	0.45	0.08

3. Numerical Results

Calculations of three variants of flat shells of double curvature were carried out, the geometric parameters of the shells are presented in Table 1.

Fixing the contour – hinged-fixed, load – static. Material – steel $(\mu_{12}=\mu_{21}=\mu=0.3,\ \ E_1=E_2=E=2.1\cdot10^5\,\text{MPa})$. Width and height of cutouts $\upsilon_\alpha=0{,}1a,\upsilon_\beta=0{,}1b,h^{\alpha\beta}=h.$ The number of cutouts in both directions is assumed to be the same.

Figure 2 shows the ratio of the volume of the cutouts V^V to the volume of the skin of the V^0 shells depending on the number of cutouts in each direction. As follows from Fig. 2, structures were accepted for calculations with the number of cutouts not exceeding 50 % of the shell volume.

The values of critical buckling loads for shells for different numbers of notches and for different numbers of terms in the expansion of the approximating N functions are presented in Table 2. On Fig. 3, the obtained values of buckling loads are presented graphically. From the graph presented in Fig. 3, it follows that the values of the calculation results for the number of terms in the expansion of the approximating functions $N=9$ and $N=16,$ in general, converge with each other.

Figure 4 shows the graphs of the dependence of the deflection W on the load q with a different number of cutouts $(0\times0,4\times4,6\times6)$ for the shell option 1. In Fig. 4, the curves W_c – deflection in the center of the structure $(x=a/2,y=b/2)$; curves W_4 – deflection in the fourth part of the $(x=a/4,y=b/4)$ design.

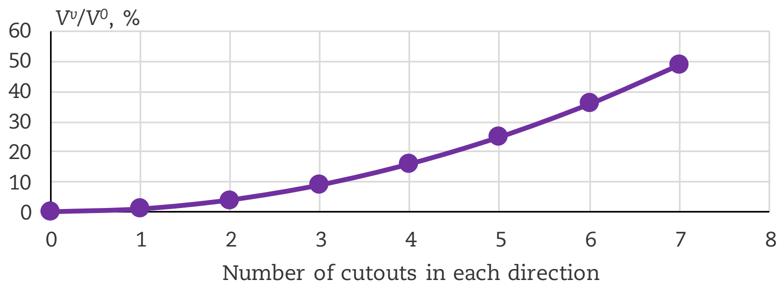

Fig. 2. The ratio of the volume of cutouts to the volume of shell skins depending on the number of cutouts in each direction.

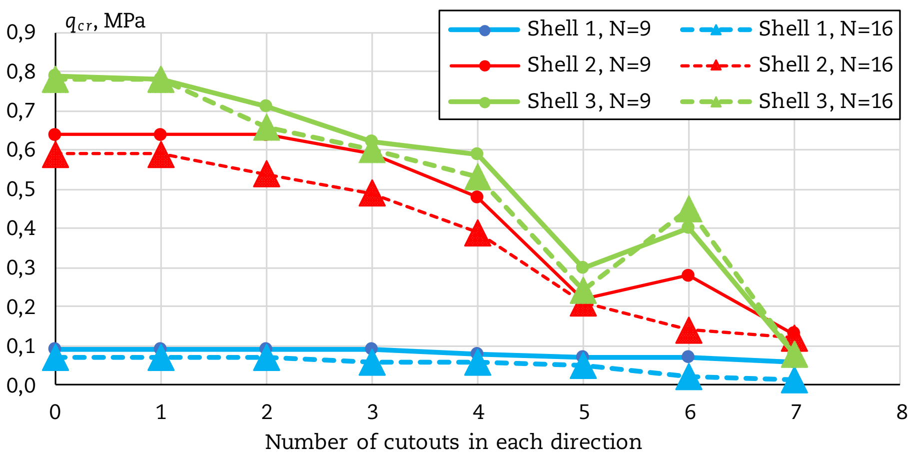

Fig. 3. Critical load values for different number of attenuations.

According to the dependence obtained, it can be seen that for the shell option 1 with the number of cutouts 0 × 0 and 4 × 4, one jump to the equilibrium state occurs. However, when the number of cutouts is 6 × 6, two jumps to the equilibrium state occur.

Figures 5 and 6 show the deflection fields of the shells of variants 2 and 3, respectively, with the number of cutouts 6×6, with the number of terms in the expansion of the approximating functions $N = 16$.

According to Fig. 5, on the left is the field of shell deflections before buckling at a load of $q = 0.14$ MPa, on the right is the field of shell deflections after buckling of the shell at a load of $q = 0.15$ MPa. According to Fig. 5, it follows that before the buckling occurs in the fourth part of the shell, the structure is bent. In this case, the greatest deflection is observed at points with coordinates $(0.1a; 0.5b)$ and $(0.4a; 0.4b)$ (similarly for symmetrical points).

After buckling, the largest deflection is in the center of the structure. In this case, dents are observed between the center and quarters of the shell, and a bulge occurs in the corners of the shell.

Based on Fig. 6, on the left is the field of shell deflections before buckling at a load of $q = 0.45$ MPa, on the right is the field of shell deflections after buckling of the shell at a load of $q = 0.46$ MPa.

According to the deflection fields shown in Fig. 6, before the buckling, the greatest value of deflections was observed in the corners of the shell. In this case, a bend is fixed in the center of the shell. After buckling, the deflection field looks similar to that shown in Fig. 5.

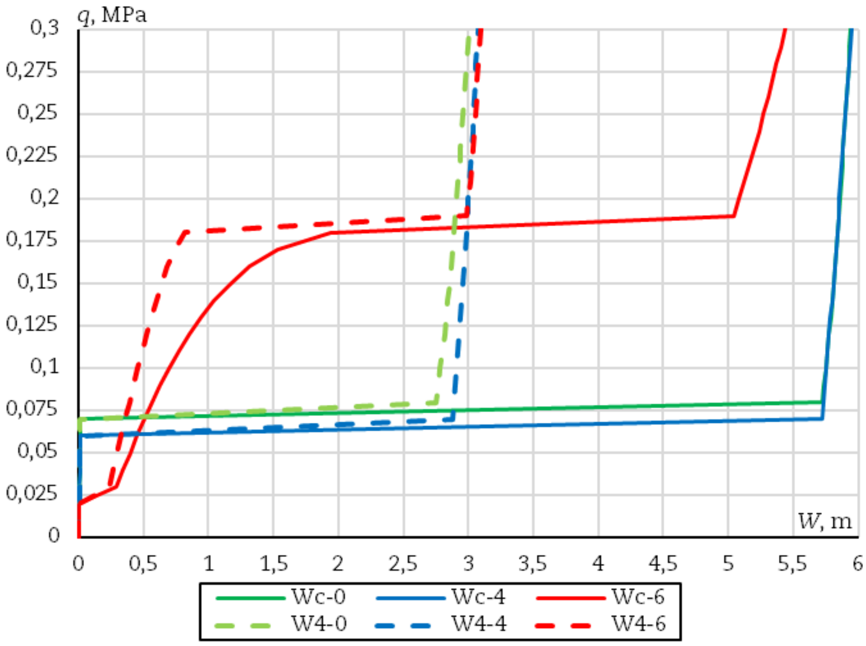

Fig. 4. Graph of deflection versus load for different number of weakening for shell option 1.

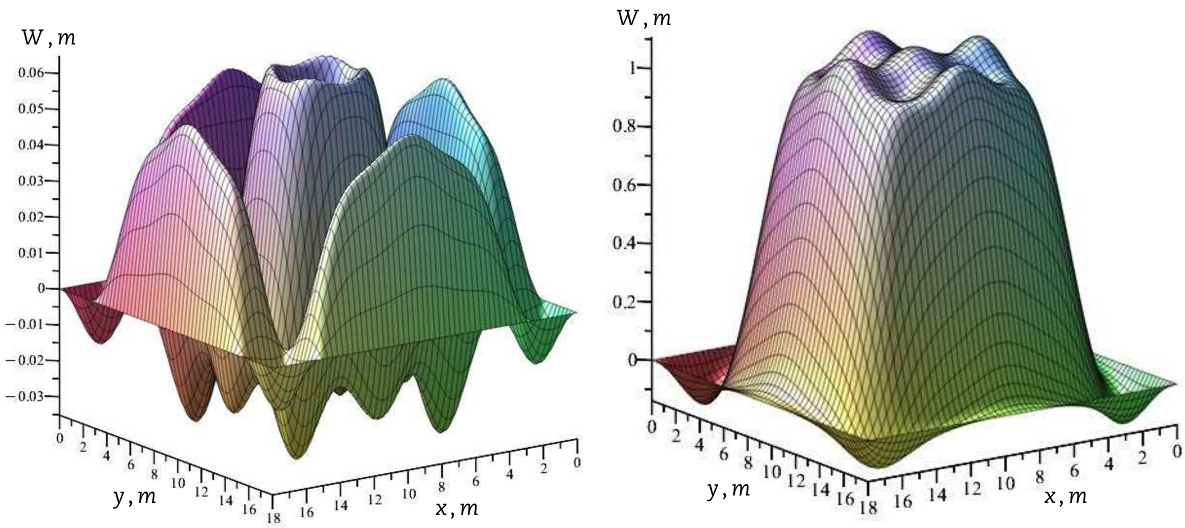

Fig. 5. Deflection fields of the shell option 2 with the number of cutouts 6×6.

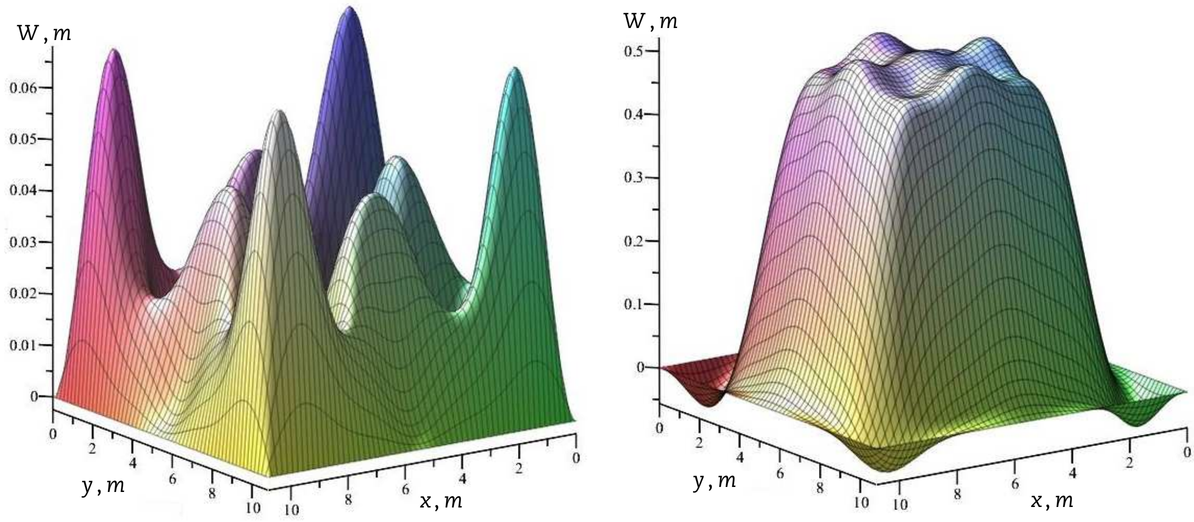

Fig. 6. Deflection fields of the shell option 3 with the number of cutouts 6×6.

Verification of the method for calculating shell structures, by comparison with other methods and experimental results, was carried out earlier in [35].

From the data obtained, it can be concluded that considering the weakening of the structure by cutouts leads to a decrease in the critical load. Moreover, when the number of cutouts is 6×6 for the options under consideration, several buckling, after which the deflection value begins to increase monotonically. Based on this, the following conclusion can be drawn: for the structures under consideration, it was found that when up to 10 % of the structure volume is switched off from work, the decrease in the critical load does not exceed 25 %.

4. Conclusion

In this work, a study of the buckling of shallow shells of double curvature was carried out, considering cutouts. The results of this research are summarized below:

- A mathematical model proposed considered the geometric nonlinearity, transverse shifts, orthotropy of the material, weakening of the structure by cutouts in the form of a functional of the total potential energy of the shell deformation.
- To study the buckling of shells under consideration, the problem of finding the minimum of the functional by the Ritz method was solved. This allowed us to reduce the problem to solving a system of nonlinear algebraic equations. The solution of the system of nonlinear algebraic equations was carried out by Newton's method.
- The mathematical model and algorithm were implemented in the Maple 2022 software package.
- Shells with square through cuts in plan (the thickness of the cut was taken equal to the thickness of the shell), evenly dispersed over the structure, were considered. The dimensions of cutouts in the plan (length and width) were taken equal to 10 % of the length and width of the shell, respectively.
- It has been established that the weakening of shells by cutouts leads to a decrease in the critical load. Shutdown of up to 10 % of the structure volume leads to a decrease in the critical load by 25 % for the shells under consideration.
- When the number of cuts is 6×6, there are several buckling of the structure, after which there is a monotonous increase in deflections.

Author Contributions

All results presented in the work are equally owned by both authors. The manuscript was written through the contribution of all authors. All authors discussed the results, reviewed, and approved the final version of the manuscript.

Acknowledgments

Not Applicable.

Conflict of Interest

The authors declared no potential conflicts of interest concerning the research, authorship, and publication of this article.

Funding

The research was supported by grant for the implementation of research work by scientific and pedagogical workers of SPbGASU in 2023.

Data Availability Statements

Not Applicable.

Nomenclature

a, b, h	Shell dimensions along x, y, z coordinates
A, B	Lame parameters describing the shell geometry;
E_1, E_2, E	Elastic moduli;
E_s	Functional of the total potential energy of the deformation of the shell structure;
E_s^0	Functional of the total potential energy of the deformation of the skin;
E_s^V	Functional of the total potential energy of the deformation of cutouts
$\bar{F}_V$	Functions characterizing the area of cutouts;
G_{12}, G_{13}, G_{23}	Shear modules;
$h^{\alpha\beta}$	Thickness of the notch;
$H^V(x, y)$	Function characterizing the location and depth of cutouts;
$\bar{J}_V$	Functions characterizing the moment of inertia of cutouts;
k_x, k_y	Main curvatures of the shell along x & y axes;
M_x, M_y, M_{xy}, M_{yx}	Moments, occurring in the structure;
$M_x^0, M_y^0, M_{xy}^0, M_{yx}^0$	Moments, occurring in the skin;
$M_x^V, M_y^V, M_{xy}^V, M_{yx}^V$	Moments, occurring in cutouts areas;
N_x, N_y, N_{xy}, N_{yx}	Forces, occurring in the structure;
$N_x^0, N_y^0, N_{xy}^0, N_{yx}^0$	Forces, occurring in the skin;
$N_x^V, N_y^V, N_{xy}^V, N_{yx}^V$	Forces, occurring in cutouts areas;
N	Number of terms in the expansion of Ritz method;
o, p	Number of cutouts along the x and y axes;
q, P_x, P_y	Load components;
q_{cr}	Critical buckling load;
Q_x, Q_y	Transverse forces in the planes xOz and yOz, occurring in the structure;
Q_x^0, Q_y^0	Transverse forces in the planes xOz and yOz, occurring in the skin;
Q_x^V, Q_y^V	Transverse forces in the planes xOz and yOz, occurring in cutouts areas;
R_1, R_2	Radii of the main curvatures;
$\bar{S}_V$	Functions characterizing the static moment of cutouts;
U, V, W	Displacement functions;
$\upsilon_\alpha, \upsilon_\beta$	Widths of cutouts in the x, y directions;
V^0	Volume of the skin;
V^V	Volume of the cutouts;
W_c	Deflection in the center of a structure;
W_4	Deflection in the quadrant of a structure;
α, β	Indices indicate the number of a rectangular cutout, the sides of which are parallel to the x and y axes
γ_{xy}	Shear deformation in the xOy plane;
$\bar{\delta}(x - x_\beta)$	Single columnar function of variable x;
$\bar{\delta}(y - y_\alpha)$	Single columnar function of variable y;
$\chi_1, \chi_2, \chi_{12}$	Functions of curvature and torsional change;
Ψ_x, Ψ_y	Functions of the normal rotation angles in the xOz and yOz planes, respectively;
$\varepsilon_x, \varepsilon_y$	Deformations of elongation along the x, y coordinates of the middle surface;
μ_{12}, μ_{21}, μ	Poisson's ratios;

References

[1] Treshchev, A., Kuznetsova, V., Study of the Influence of the Kinetics of Hydrogen Saturation on the Stress-Deformed State of a Spherical Shell Made from Titanium Alloy, *International Journal for Computational Civil and Structural Engineering*, 18(2), 2022, 121–130. DOI: 10.22337/2587-9618-2022-18-2-121-130.

[2] Razov, I., Sokolov, V., Dmitriev, A., Ogorodnova, J., Parametric vibrations of the underground oil pipeline, *E3S Web of Conference*; ed. Malygina I., 363, 2022, 01038. DOI: 10.1051/e3sconf/202236301038.

[3] Kayumov, R.A., Shakirzyanov, F.R., *Large Deflections and Stability of Low-Angle Arches and Panels During Creep Flow*, Multiscale Solid Mechanics; ed. Altenbach H., Eremeyev V.A., Igumnov L.A., Cham: Springer International Publishing, 141, 2021, 237–248. DOI: 10.1007/978-3-030-54928-2_18.

[4] Kamenev, I.V., Semenov, A.A., Rationale of the use of the constructive anisotropy method in the calculation of shallow shells of double curvature, weakened holes, *PNRPU Mechanics Bulletin*, 2, 2016, 54–68. DOI: 10.15593/perm.mech/2016.2.05. (in Russian)

[5] Karpov, V.V., Models of the shells having ribs, reinforcement plates and cutouts, *International Journal of Solids and Structures*, 146, 2018, 117–135. DOI: 10.1016/j.ijsolstr.2018.03.024.

[6] Solovei, N.A., Krivenko, O.P., Malygina, O.A., Finite element models for the analysis of nonlinear deformation of shells stepwise-variable thickness with holes, channels and cavities, *Magazine of Civil Engineering*, 1(53), 2015, 56–69. DOI: 10.5862/MCE.53.6. (in Russian)

[7] Zakharova, Yu.V., Lokhmatova, L.G., Simulation of stress-strain state of defected composite shells, *Engineering Journal: Science and Innovation*, 11(59), 2016. DOI: 10.18698/2308-6033-2016-11-1552. (in Russian)

[8] Zhao, C., Niu, J., Zhang, Q., Zhao, C., Xie, J., Buckling behavior of a thin-walled cylinder shell with the cutout imperfections, *Mechanics of Advanced Materials and Structures*, 26(18), 2019, 1536–1542. DOI: 10.1080/15376494.2018.1444225.

[9] Dmitriev, V.G., Egorova, O.V., Zhavoronok, S.I., Rabinskii, L.N., Investigation of Buckling Behavior for Thin-Walled Bearing Aircraft Structural Elements with Cutouts by Means of Numerical Simulation, *Russian Aeronautics*, 61(2), 2018, 165–174. DOI: 10.3103/S1068799818020034.

[10] Yılmaz, H., Kocabaş, İ., Özyurt, E., Empirical equations to estimate non-linear collapse of medium-length cylindrical shells with circular cutouts, *Thin-Walled Structures*, 119, 2017, 868–878. DOI: 10.1016/j.tws.2017.08.008.

[11] Xia, Y., Wang, H., Zheng, G., Shen, G., Hu, P., Discontinuous Galerkin isogeometric analysis with peridynamic model for crack simulation of shell structure, *Computer Methods in Applied Mechanics and Engineering*, 398, 2022, 115193. DOI: 10.1016/j.cma.2022.115193.

[12] Ambati, M., Heinzmann, J., Seiler, M., Kästner, M., Phase-field modeling of brittle fracture along the thickness direction of plates and shells, *International Journal for Numerical Methods in Engineering*, 123(17), 2022, 4094–4118. DOI: 10.1002/nme.7001.

[13] Wang, Y., Hu, J., Kennedy, D., Wang, J., Wu, J., Adaptive mesh refinement for finite element analysis of the free vibration disturbance of cylindrical shells due to circumferential micro-crack damage, *Engineering Computations*, 39(9), 2022, 3271–3295. DOI: 10.1108/EC-09-2021-0555.

[14] Giani, S., Hakula, H., Free vibration of perforated cylindrical shells of revolution: Asymptotics and effective material parameters, *Computer Methods in Applied Mechanics and Engineering*, 403, 2023, 115700. DOI: 10.1016/j.cma.2022.115700.

[15] Arbelo, M.A., Herrmann, A., Castro, S.G.P., Khakimova, R., Zimmermann, R., Degenhardt, R., Investigation of Buckling Behavior of Composite Shell Structures with Cutouts, *Applied Composite Materials*, 22(6), 2015, 623–636. DOI: 10.1007/s10443-014-9428-x.

[16] Gangadhar, L., Kumar, T.S., Finite Element Buckling Analysis of Composite Cylindrical Shell with Cutouts Subjected to Axial Compression, *International Journal of Advanced Science and Technology*, 89, 2016, 45–52. DOI: 10.14257/ijast.2016.89.06.

[17] Shen, K.-C., Yang, Z.-Q., Jiang, L.-L., Pan, G., Buckling and Post-Buckling Behavior of Perfect/Perforated Composite Cylindrical Shells under Hydrostatic Pressure, *Journal of Marine Science and Engineering*, 10(2), 2022, 278. DOI: 10.3390/jmse10020278.

[18] Ghanbari Ghazijahani, T., Jiao, H., Holloway, D., Structural behavior of shells with different cutouts under compression: An experimental study,

Journal of Constructional Steel Research, 105, 2015, 129–137. DOI: 10.1016/j.jcsr.2014.10.020.
[19] Krishna, G.V., Narayanamurthy, V., Viswanath, C., Buckling behaviour of FRP strengthened cylindrical metallic shells with cut-outs, *Composite Structures*, 300, 2022, 116176. DOI: 10.1016/j.compstruct.2022.116176.
[20] Sohan, R., Likith, S., Sai, J., Vadlamani, S., Linear, nonlinear and post buckling analysis of a stiffened panel with cutouts, *IOP Conference Series: Materials Science and Engineering*, 1248(1), 2022, 012078. DOI: 10.1088/1757-899X/1248/1/012078.
[21] da Silveira, T., Pinto, V., Neufeld, J.P., Pavlovic, A., Rocha, L., dos Santos, E., Isoldi, L.A., Applicability Evidence of Constructal Design in Structural Engineering: Case Study of Biaxial Elasto-Plastic Buckling of Square Steel Plates with Elliptical Cutout, *Journal of Applied and Computational Mechanics*, 7(2), 2021, 922–934. DOI: 10.22055/jacm.2021.35385.2647.
[22] Keshav, V., Patel, S.N., Kumar, R., Watts, G., Effect of Cutout on the Stability and Failure of Laminated Composite Cylindrical Panels Subjected to In-Plane Pulse Loads, *International Journal of Structural Stability and Dynamics*, 22(08), 2022, 2250087. DOI: 10.1142/S0219455422500870.
[23] Dewangan, H.C., Panda, S.K., Hirwani, C.K., Numerical deflection and stress prediction of cutout borne damaged composite flat/curved panel structure, *Structures*, 31, 2021, 660–670. DOI: 10.1016/j.istruc.2021.02.016.
[24] Dewangan, H.C., Sharma, N., Panda, S.K., Thermomechanical loading and cut-out effect on static and dynamic responses of multilayered structure with TD properties, *Proceedings of the Institution of Mechanical Engineers, Part C: Journal of Mechanical Engineering Science*, 236(16), 2022, 9081–9094. DOI: 10.1177/09544062221089153.
[25] Li, Q., Wang, D.F., Influence of cutout position on buckling of large-scale thin-walled cylindrical shell of desulphurizing tower with welding induced imperfection under wind loading, *Applied Mechanics and Materials*, 687–691, 2014, 68–72. DOI: 10.4028/www.scientific.net/AMM.687-691.68.
[26] Labans, E., Bisagni, C., Celebi, M., Tatting, B., Gürdal, Z., Blom-Schieber, A., Rassaian, M., Wanthal, S., Bending of Composite Cylindrical Shells with Circular Cutouts: Experimental Validation, *Journal of Aircraft*, 56(4), 2019, 1534–1550. DOI: 10.2514/1.C035247.
[27] Gokyer, Y., Sonmez, F.O., Topology optimization of cylindrical shells with cutouts for maximum buckling strength, *Journal of the Brazilian Society of Mechanical Sciences and Engineering*, 45(1), 2023, 13. DOI: 10.1007/s40430-022-03941-w.
[28] Groh, R.M.J., Wu, K.C., Nonlinear Buckling and Postbuckling Analysis of Tow-Steered Composite Cylinders with Cutouts, *AIAA Journal*, 60(9), 2022, 5533–5546. DOI: 10.2514/1.J061755.
[29] Shahani, A.R., Kiarasi, F., Numerical and Experimental Investigation on Post-buckling Behavior of Stiffened Cylindrical Shells with Cutout subject to Uniform Axial Compression, *Journal of Applied and Computational Mechanics*, 9(1), 2023, 25–44. DOI: 10.22055/jacm.2021.33649.2261.
[30] Li, Z., Cao, Y., Pan, G., Influence of geometric imperfections on the axially loaded composite conical shells with and without cutout, *AIP Advances*, 10(9), 2020, 095106. DOI: 10.1063/5.0021103.
[31] Kamaloo, A., Jabbari, M., Tooski, M.Y., Javadi, M., Nonlinear Free Vibrations Analysis of Delaminated Composite Conical Shells, *International Journal of Structural Stability and Dynamics*, 20(01), 2020, 2050010. DOI: 10.1142/S0219455420500108.
[32] Kumar Chaubey, A., Kumar, A., Chakrabarti, A., Effect of multiple cutouts on shear buckling of laminated composite spherical shells, *Materials Today: Proceedings*, 21, 2020, 1155–1163. DOI: 10.1016/j.matpr.2020.01.065.
[33] Juhász, Z., Szekrényes, A., An analytical solution for buckling and vibration of delaminated composite spherical shells, *Thin-Walled Structures*, 148, 2020, 106563. DOI: 10.1016/j.tws.2019.106563.
[34] Semenov, A.A., Moskalenko, L.P., Karpov, V.V., Sukhoterin, M.V., Buckling of cylindrical panels strengthened with an orthogonal grid of stiffeners, *Bulletin of Civil Engineers*, 6(83), 2020, 117–125. DOI: 10.23968/1999-5571-2020-17-6-117-125. (in Russian)
[35] Karpov, V.V., Semenov, A.A., Refined model of stiffened shells, *International Journal of Solids and Structures*, 199, 2020, 43–56. DOI: 10.1016/j.ijsolstr.2020.03.019.

ORCID iD

Nikolai Mishurenko https://orcid.org/0000-0002-0022-734X
Alexey Semenov https://orcid.org/0000-0001-9490-7364

How to cite this article: Mishurenko N., Semenov A. Influence of Discretely Introduced Cutouts on the Buckling of Shallow Shells with Double Curvature, *J. Appl. Comput. Mech.*, 10(1), 2024, 55–63. https://doi.org/10.22055/jacm.2023.44219.4182